Study of Interfacial Charge-Transfer Complex on TiO_2 Particles in Aqueous Suspension by Second-Harmonic Generation

Yan Liu, J. I. Dadap, David Zimdars, and Kenneth B. Eisenthal*

Department of Chemistry, Columbia University, New York, New York 10027

Received: October 27, 1998; In Final Form: January 20, 1999

We report the first direct observation of an interfacial charge-transfer complex using second-harmonic spectroscopy. The second-harmonic spectrum of catechol adsorbed on 0.4 micron-sized TiO_2 (anatase) colloidal particles in aqueous suspension reveals a charge-transfer band centered at 2.72 eV (456 nm). In addition, the adsorption isotherm of catechol on the colloidal TiO_2 suspension was obtained and gave an excellent fit to the Langmuir adsorption model. From this, we infer the free energy of the adsorption to be $\Delta G° = -6.8$ kcal/mol.

1. Introduction

Titanium dioxide (TiO_2) is a wide band-gap semiconductor having two common crystal forms: rutile and anatase. Due to its high physical and chemical stability, it is extensively studied as a photocatalyst for photolysis of water,[1,2] and for oxidative photomineralization of organic pollutants in wastewater[3], aimed at harvesting solar energy. Colloidal TiO_2 particles have been used in many of these studies[3−7] mainly to take advantage of the huge specific surface area of small particles. TiO_2 has three band-gap transitions; for rutile and anatase the exact position of the transitions are slightly different, but there are two indirect transitions at approximately 3.0 and 3.2 eV, while there is a direct transition at 3.7 eV.[8,9] Because these transitions are in the UV region, the solar energy conversion efficiency of TiO_2 is limited.

Surface photosensitization is a very important process in the attempt to utilize solar energy by wide band-gap semiconductors[5−8,10−19]. As the dye adsorbs on the semiconductor surface, it can form a surface complex with the semiconductor. If there is suitable energy−band match between the excited state of the surface complex with the conduction band of the semiconductor, the surface complex can be excited by visible light, which will then inject an electron into the conduction band of the semiconductor (Scheme 1). In some cases, an electron is transferred from the HOMO of an adsorbed molecule to the valence band of the photoexcited semiconductor. In this case, the molecule (often a pollutant) is photooxidized. Thus a series of charge-transfer reactions can be induced. The surface charge-transfer process had been confirmed and studied by transient absorption spectroscopy,[17−21] fluorescence quenching,[22−26] and surface redox reactions of a number of small molecules[27,28] and ions.[29,30]

It is well-known that catechol, together with some other organic small molecules of similar structures, such as salicylic acid,[28] alizarin,[32] and coumarin 343,[24,32,33] can form charge-transfer complexes on TiO_2 surfaces. The large spectral changes of the catechol adsorbed on TiO_2 surfaces compared with the spectra of free catechol in solution and that of TiO_2 has been observed for nanometer-sized particle suspensions by UV/vis transmittance measurements,[28] and for dried powders by diffuse reflectance measurements.[31] The broad absorbance peak around 420−430 nm with a tail extending to 600 nm has been assigned to the intramolecular ligand-to-titanium charge-transfer transition within the surface complex.[28,31]

SCHEME 1

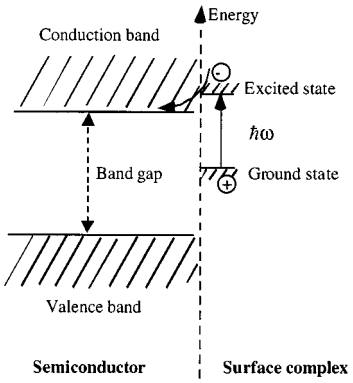

Catechol in aqueous solution has a strong but narrow $\pi-\pi^*$ transition at 275 nm, and no absorbance above 300 nm. It can form a complex with an aqueous Ti(IV) ion with an absorbance around 390 nm.[34] Because of the broken bonds on the crystal surfaces, there are valence-unfilled Ti(IV) centers and O(II) centers. In aqueous solution, the water molecules are dissociatively adsorbed on the TiO_2 surface, which results in the H^+ ion associating with the di-coordinated surface O atom forming acidic $\equiv OH^{1/3+}$, while the OH^- ion associating with the pentacoordinated surface Ti atom forming basic $\equiv TiOH^{1/3-}$, respectively.[31,35] In the catechol−TiO_2 surface reaction, the −OR groups in catechol substitute for the −OH groups in the basic $\equiv TiOH^{1/3-}$, thereby forming the surface complex.

The spectrum and the population of the surface complex are important to any description of the photochemistry and photophysics of the system. Previous linear optical measurements on tens of nanometer-sized TiO_2 particles, revealed the existence of a charge-transfer band near 420 nm, appearing as a shoulder in a UV/vis diffuse reflectance spectrum on a TiO_2-catechol nanoparticle powder[28] and a UV/vis absorption spectrum by a TiO_2 nanoparticle suspension in aqueous catechol solution[31]. Because of the small size of the particles, UV/vis measurements are not limited by scattering despite the relatively large refractive

* Author to whom correspondence should be addressed.

10.1021/jp984288e CCC: $18.00
Published on Web 03/12/1999

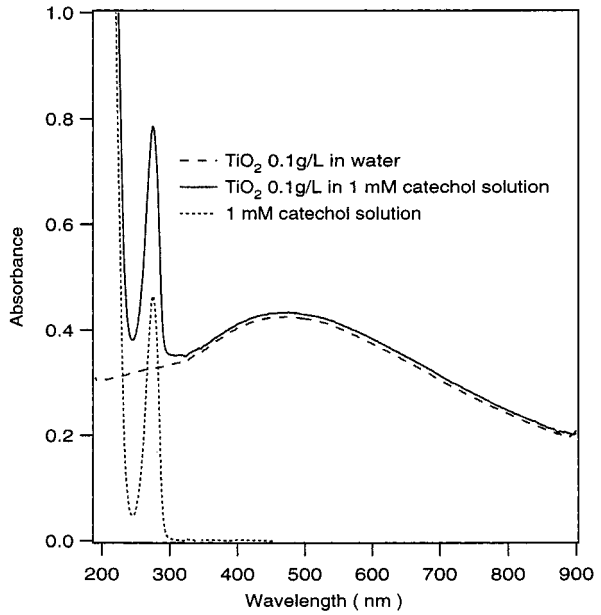

Figure 1. The UV/vis spectra of TiO_2 0.1 g/L (particle density $\approx 8 \times 10^8$ cm^{-3}) suspension in water and in 1 mM catechol solution using a 0.2 cm path length quartz cuvette. The spectrum of 1 mM catechol solution is also shown for comparison. For the two suspension samples, the broad peak $\sim$ 470 nm is due to the Mie-scattering of the submicron size particles. For the mixture sample, no interfacial charge transfer band can be detected by the linear UV/vis scattering because of the relatively low density of the surface complex.

index of TiO_2, $n \sim 2.7$. This makes it possible to use a high density of nanoparticles to increase the signal.

However for larger particle sizes, comparable to the wavelength of the optical probe, turbidity can dominate the absorbance signal and thereby obscure the charge-transfer band as shown in Figure 1. This will be discussed in more detail later. We now summarize the results obtained for the nanoparticle-catechol surface complex.

Rodriguez et al.[31] measured the UV/vis differential diffuse reflectance spectrum of vacuum-dried 30-nm powders of TiO_2 (anatase) with adsorbed catechol, and observed the charge-transfer transition. In that study, the spectrum of the dried powder was measured, not that of the aqueous suspension. The environment of the catechol/TiO_2 complex differs considerably for these two cases. The adsorption isotherm of catechol in a TiO_2 particle suspension was obtained by potentiometric titration of the surface OH$-$ group of TiO_2 particles by HCl, in conjunction with conventional methods of studying the surface adsorption of solid particles from a solution, which include mixing, separation, and detection steps. The equilibrium constant for the adsorption was obtained from a Langmuir fit as $K_{eq} = 8 \times 10^3$ L mol^{-1}, corresponding to a monolayer catechol density of 1.25 μmol m^{-2}, and a free energy of $\Delta G^\circ = -7.7$ kcal/mol. They proposed the following mechanism to describe the adsorption:

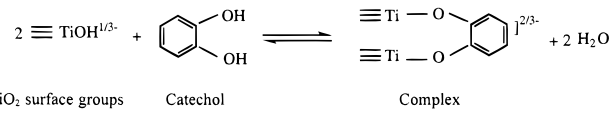

An earlier but similar study of surface complexation of 13-nm TiO_2 particles by catechol using a less polar aqueous solution of 10% methanol by volume, was performed by Moser et al.[31] A UV/vis absorption spectra reveals the existence of a charge-transfer band appearing as a shoulder near 420 nm. The adsorption equilibrium constant for this system was obtained from a Langmuir fit as $K_{eq} = 8 \times 10^4$ L mol^{-1}. This corresponds to a monolayer catechol density of 1.0 μmol m^{-2}, and a free energy of $\Delta G^\circ = -9.0$ kcal/mol, which differs considerately from the results on the catechol$-TiO_2$ powder.

In these earlier studies of catechol adsorption onto the TiO_2 surface, the surface concentration was obtained through several processes: mixing, separation, and detection. First, the particles and the adsorbate solution of known concentration are mixed. Second, after equilibration, the particles with the adsorbed molecules are then separated, e.g., by centrifugation. Finally, the supernatant and the particles are studied separately. The decrease in the adsorbate concentration in the supernatant is then used to calculate the surface excess on the particles. In this procedure, a very high density of nanoparticles was used.

In our study, we can directly probe the system in situ using second-harmonic generation (SHG), and importantly perform the measurements at sufficiently low particle densities such that we are observing only single particle effects. In other words, at low densities interparticle interactions can be neglected. Recently, we have employed this technique to selectively study the surfaces of micron- and submicron-sized particles in suspensions. Taking advantage of both the surface specificity and spectroscopic selectivity of SHG, we have studied aqueous suspensions of polystyrene beads,[36,37] liposomes,[38] semiconductor particles,[39] clay particles,[40] and oil/water emulsions,[37,41] obtaining information on the interface adsorbate populations, the free energies of adsorption, the electrostatic potential at the surface of microparticles when they are charged,[41] and the real time measurement of molecular transport across the bilayer of liposomes.[38]

Under the dipole approximation, SHG is forbidden in centrosymmetric media, e.g., in bulk solutions.[42] Because surfaces are intrinsically noncentrosymmetric, SHG becomes dipole-allowed and is thus surface specific. Although a spherical particle is centrosymmetric overall, the local regions of the microscopic surface are not. Thus the surface yields a net macroscopic nonlinear polarization provided certain conditions are satisfied. For instance when the particle is much smaller than the wavelength of light, all of the molecules on the particle surface experience the same optical field, but because of the overall centrosymmetry, there are oppositely oriented molecules on the opposite sides of the sphere. These oppositely oriented molecules have oppositely directed second-order polarizations, which result in the net second-harmonic and sum-frequency polarizations being zero. On the other hand, when the particle is comparable to the wavelength of light, the induced second-order polarizations at the front- and backsides of the particle are not opposite, so that the net second-order polarization induced by the incident light does not necessarily vanish. In addition, resonance enhancement of SHG can be achieved when either the fundamental frequency, ω, or the SH, 2ω, is in resonance with the transition of the surface species, making SHG a species-selective method.

In this study, we present the first spectroscopic SH measurement of an interfacial charge-transfer complex using catechol adsorbed on colloidal TiO_2 (anatase) particles. The SH spectrum reveals a charge-transfer band centered at 2.72 eV (456 nm) and a line width of 0.25 eV, which is different from the results obtained for both the nanoparticle catechol$-TiO_2$ powder[31] and the nanoparticle catechol$-TiO_2$ aqueous methanol suspension.[28] In addition, measurement of the uptake curve of catechol in the colloidal TiO_2 aqueous suspension yielded an equilibrium

constant, $K_{eq} = 2.1 \times 10^3$ L mol^{-1}, and an adsorption free energy $\Delta G^\circ = -6.8$ kcal/mol.

SHG has been used to study planar rutile TiO_2 surfaces, particularly in work by Schultz et al.,[43,44] on the adsorption of H_2O and O_2 on TiO_2 at vacuum−solid interface, and by Lantz et al.,[45−47] on the space-charge layer that extends as far as ∼1 μm into the bulk of TiO_2 at a liquid−solid interface. In these studies, rutile was employed because of its centrosymmetry. Anatase, on the other hand, is noncentrosymmetric and the bulk SHG can dominate the surface response in macroscopic size crystals. However, for a suspension of small particles, the relative large surface area to bulk volume ratio can result in the surface SH from the adsorbates being comparable to or even greater than the bulk SH contribution. Operating at wavelengths far from the bulk resonance but close to the surface charge-transfer complex resonance further amplifies the contribution from the surface relative to the bulk. As we shall see, we separate the contributions arising from the surface and the bulk responses by taking into account their relative phase.[48] Thus, performing SH measurements on anatase instead of rutile particles allows us to compare our SH results directly with previous linear optical measurements.

2. Experiment

TiO_2 (>99% anatase) in powder form and catechol (>99%) were purchased from Aldrich and were used as received. The particle size of TiO_2 (anatase) was 0.4 μm. The TiO_2 powder was dispersed in double-distilled water by mild sonication for about 30 min. For a particle concentration of 0.1 g/L, the particle density is about 8×10^8 particles/cm^3. At this low particle density, the interactions between particles and any interference effects between particles can be neglected. Catechol solutions were made in double-distilled water, flushed with argon to avoid oxidation, and were always used within 2 days.

The samples of catechol with TiO_2 were prepared by mixing the catechol solutions with the TiO_2 dispersion. Care was taken to minimize exposure to air and light. The mixture samples, at pH ∼ 6.5, were all sealed and kept overnight in the dark to ensure adsorption equilibrium. Because the point of zero charge of TiO_2 surface is near pH 6.5 ($pK_{a1} = 5.0$, $pK_{a2} = 7.8$),[49] and catechol is a very weak diprotic acid ($pK_{a1} = 9.2$, $pK_{a2} = 13.0$), both the TiO_2 surface and the catechol molecules in solution are neutral at pH ∼ 6.5.

The setup for the second-harmonic measurements has been described in detail elsewhere.[36,37] Briefly, a Ti:sapphire laser pumped by an Ar ion laser provided 100 fs pulses at an 82 MHz repetition rate, tunable between 750 nm to 920 nm with a typical bandwidth ∼ 10 nm. The average power was in the range 1.3−1.5 W. The fundamental light was focused into a 0.2 cm path length quartz cuvette. The second harmonic photons in the transmitted (forward) direction were collected by a lens (focal length 5 cm, diameter 10 cm) and passed through a thin film polarization analyzer to a monochromator. The SH signal was recorded using single photon counting. An IR-transmitting, UV-blocking filter was placed before the sample to get rid of spurious SH prior to the sample; an IR-blocking, UV-transmitting filter was placed after the sample to cut off the fundamental light while transmitting SH. We estimate ∼1000 TiO_2 particles within the focal volume of the laser beam.

A series of UV/vis spectral absorbance measurements (Perkin−Elmer, Lambda 9) demonstrated the stability of the TiO_2 suspension over a period of several hours. Before and after the experiment, the UV/vis spectra changed by <1%, indicating no aggregation or other changes during the experiment. The UV spectra of the catechol−water solution for a series of concentrations showed that the absorbance of catechol solution at the absorbance peak wavelength, 275 nm, obeys Beer−Lambert's law up to 6 mM. For concentrations greater than 6 mM, the absorbance vs concentration curve deviated from a straight line. For this reason the adsorption isotherm measurements were carried out for catechol concentrations less than 6 mM.

Typical UV/vis spectra are shown in Figure 1, for a pure 1 mM catechol solution (dotted line), a 0.1 g/L suspension of TiO_2 in water (dashed line), and a 0.1 g/L suspension of TiO_2 in 1 mM catechol solution (solid line) in a 0.2 cm path length cuvette. Note that the TiO_2−catechol optical density is simply the sum of the individual TiO_2 suspension and catechol solution optical densities. The broad peak at ∼470 nm arises from the Mie-scattering of the submicron TiO_2 particles. Also note that for this mixture, no charge-transfer band is detectable from this UV/vis measurement because of the low density of the surface complexes and the relatively large size of the particles that are responsible for the large turbidity. To estimate the optical density of our catechol−TiO_2 charge-transfer band near 400 nm, we make use of the results of Moser et al.,[28] where ϵ(400 nm) ≈ 5×10^4 M^{-1} cm^{-1} and the monolayer catechol density ∼1 μmol/m^2. For 0.4 μm size particles, at a particle density of 8×10^8/cm^3, the catechol bulk depletion is ∼0.4 μM. Hence for a 0.2 cm path length the optical density due to the charge-transfer band is OD ≈ 0.004, a value that is very small compared to the OD ≈ 0.4 arising from scattering. In contrast, the results of Moser et al.[28] and Rodriguez et al.[31] on TiO_2 nanoparticles indicate bulk depletion of the order of 1 mM. The large specific surface area, high particle density, and low turbidity make the charge-transfer band observable in these latter linear optical experiments.

3. Results and Discussions

a. Second-Order Nonlinear Light Scattering. With a fixed fundamental laser frequency of 818 nm, the spectra of the second-order light scattering were taken by changing the wavelength setting of the monochromator for the following samples: (1) 5 mM catechol aqueous solution, (2) 0.1 g/L TiO_2 suspension in water, and (3) 0.1 g/L TiO_2 suspension in 5 mM catechol, Figure 2. The polarizations of the incident fundamental light and the output SH were set and detected along the vertical direction with respect to the laboratory frame. We denote this polarization configuration as V-in/V-out.

The SH spectrum of 5 mM catechol water solution irradiated with 818 nm light coincides with the spectrum of neat water (not shown) in the wavelength range 390−460 nm, and for all catechol concentrations used. This is expected because the catechol is nonresonant in the fundamental and SH wavelength ranges. The small bump at 2ω is due to the hyper-Rayleigh scattering from bulk water, which arises from the density and orientational fluctuations of the water molecules. The broad peak to the red of 2ω is determined to be a hyper-Raman signal, whose peak position shifts as the fundamental light wavelength is shifted.

The anatase suspension in water, on the other hand, yields a strong signal at 2ω that comprises SH from the water/TiO_2 interface and the TiO_2 bulk (because of its noncentrosymmetry[50,51]), and a small hyper-Rayleigh signal from water. We believe that the total signal arises mainly from the bulk on the basis of the following considerations. First, anatase is noncentrosymmetric, hence the bulk nonlinearity is expected to be much larger than the TiO_2/aqueous interface contribution. We can

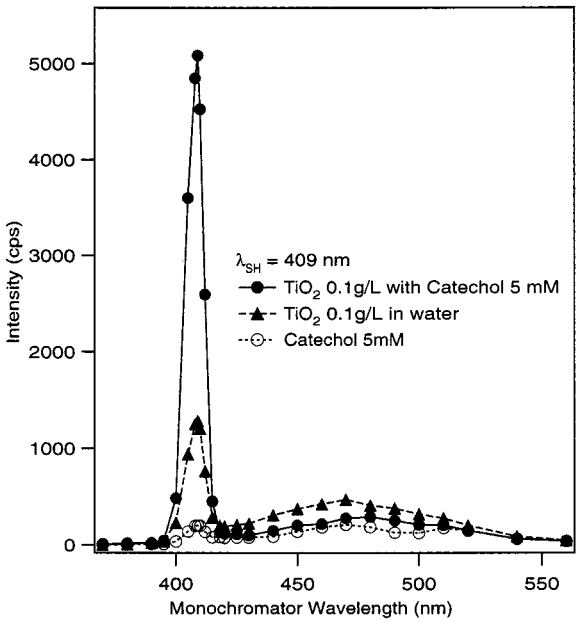

Figure 2. The spectra of second-order light scattering at a pump wavelength of 818 nm. Both the fundamental and the SH light are vertically polarized relative to the laboratory frame.

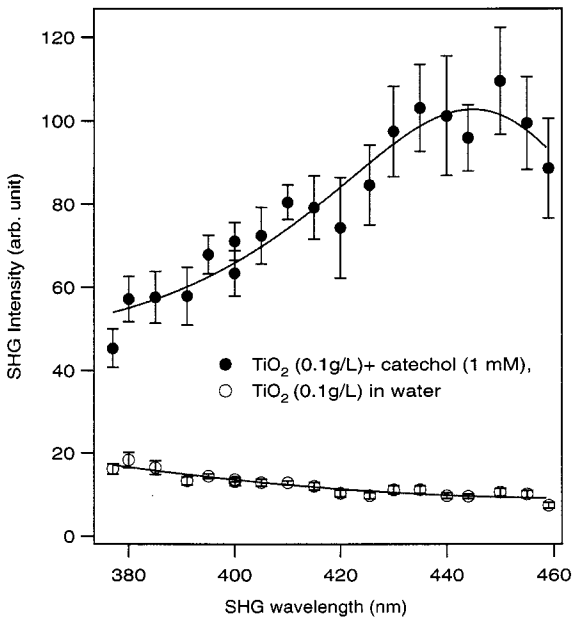

Figure 3. The turbidity-corrected and normalized SH spectra of TiO_2 in water and TiO_2 in 1 mM catechol solution. The peak of the catechol−TiO_2 surface complex band is at $\lambda_{max} = 456 \pm 4$ nm.

estimate the nonlinear susceptibility of bulk TiO_2 relative to quartz using Miller's rule,[52] which yields a large value of $|\chi^{(2)}_{TiO_2}| \approx 150|\chi^{(2)}_{quartz}|$, where we made use of the following refractive indices: $n^{800nm}_{TiO_2} = 2.6$, $n^{400nm}_{TiO_2} = 2.7$, $n^{800nm}_{quartz} = 1.45$, and $n^{400nm}_{quartz} = 1.47$.[53,54] Second, if this component originates primarily from the bulk, any interfacial modification should not affect the signal at 2ω. The pH dependence of SHG from a TiO_2 suspension was measured. Varying the pH from pH = 2 to pH = 12 modifies the surface charge of TiO_2 whose zero-point charge occurs at pH ≈ 6.5. However, no changes were observed in the SH signal within experimental uncertainty, implying that the contributions from the surface as well as from the polarization of water molecules near the interface are negligible compared to the bulk response. Hence, the extraction of the catechol−TiO_2 surface complex signal from the total SH is simplified. The surface complex signal can be observed because of its near resonance with the SH wavelength, which enhances the surface complex signal relative to the bulk contribution.

The TiO_2 suspension with 5 mM catechol gave a strong signal at the second-harmonic wavelength, 409 nm. This signal contains three parts: the SH from the surface complex of TiO_2 with catechol, the SH due from the bulk of the TiO_2 particles, and a small hyper-Rayleigh signal from water bulk. Because the water hyper-Rayleigh signal is incoherent, it can be easily separated from the coherent SH signal. If the turbidity introduced by the particles is taken into account, the total signal is simply the sum of the coherent SH signal and the hyper-Rayleigh. One issue remains—the separation of the catechol−TiO_2 surface complex and the bulk TiO_2 signals. To separate these two contributions, knowledge of the relative phase between them is necessary.

b. Theoretical Considerations. The TiO_2 0.4 micron size suspensions were turbid in the wavelength range of ω and 2ω so that the intensities of the fundamental and the SH light for both the catechol−TiO_2 mixture and the TiO_2 suspension were attenuated by light scattering. Hence, the raw signals were first corrected for turbidity at both ω and 2ω. This correction was performed by dividing the observed SH signal by a factor that is obtained by integrating the SH intensity along the path length of the laser light, taking into account the attenuation of light by the measured optical densities at both the fundamental and the SH frequencies.[41] The turbidity-corrected signal at 2ω for these two samples can be written as follows:

$$I^{(2\omega)}_{tot} = I^{HR}_{H_2O} + |E^{SH}_{TiO_2} + E^{SH}_{cat-TiO_2}|^2 \quad (1)$$

for the TiO_2−catechol suspension and

$$I^{(2\omega)}_{H_2O+TiO_2} = I^{HR}_{H_2O} + |E^{SH}_{TiO_2}|^2 \quad (2)$$

for the TiO_2 suspension alone, where $I^{HR}_{H_2O}$ is the hyper-Rayleigh intensity signal from water, $E^{SH}_{cat-TiO_2}$ and $E^{SH}_{TiO_2}$, represent the SH field contributions from the catechol−TiO_2 mixture, and the TiO_2 suspension, respectively. If the particle densities of the two samples are equal, the $E^{SH}_{TiO_2}$ terms in eqs 1 and 2 can be considered equal because the TiO_2 bulk contributes equally for both samples. Because water does not absorb in the range of ω to 2ω, its hyper-Rayleigh signal was used as a normalization standard to account for any variations in the laser intensity, pulse width, and the collection efficiency as the laser fundamental wavelength was tuned from 750−920 nm. To normalize the signal, we divide both sides of eq 1 by the hyper-Rayleigh signal, $I^{HR}_{H_2O}$, at each wavelength, yielding

$$\frac{I^{(2\omega)}_{tot}}{I^{HR}_{H_2O}} - 1 = \frac{\left||E^{SH}_{TiO_2}| + |E^{SH}_{cat-TiO_2}|e^{i\varphi}\right|^2}{I^{HR}_{H_2O}} \quad (3)$$

where φ is the relative phase between the catechol−TiO_2 and bulk TiO_2 SH fields. It should be noted in eq 3 that the SH fields, SH intensities, and the phase φ are wavelength dependent. The hyper-Rayleigh term, $I^{HR}_{H_2O}$, is not wavelength sensitive because we are far from any water resonance.

The normalized TiO_2 signal, $I^{norm}_{TiO_2} \equiv |E^{SH}_{TiO_2}|^2/I^{HR}_{H_2O}$, gradually increases as the SH wavelength, λ_{SH}, varies from 460 to 375 nm, as shown by the unfilled-circle data of Figure 3. This

gradual increase arises from the tail of the direct band-gap transition at 3.7 eV (330 nm). Because both fundamental and SH wavelengths remain far from the direct transition resonance, we approximate and empirically fit $I^{\text{norm}}_{\text{TiO}_2}$ by a real, second-order polynomial,

$$I^{\text{norm}}_{\text{TiO}_2}(\lambda_{\text{SH}}) = a_0 + a_1\lambda_{\text{SH}} + a_2\lambda^2_{\text{SH}} \tag{4}$$

The Figure 3 filled-circle data of the SH signal from the catechol and TiO_2 suspension show the existence of a resonance peak near 450 nm, which we attribute to the catechol$-TiO_2$ surface complex band. The normalized SH field of the catechol$-TiO_2$ $E^{\text{norm}}_{\text{cat}-\text{TiO}_2} \equiv E^{\text{SH}}_{\text{cat}-\text{TiO}_2}/\sqrt{I^{\text{HR}}_{\text{H}_2\text{O}}}$, can be expressed as

$$E^{\text{norm}}_{\text{cat}-\text{TiO}_2} = a + \frac{b}{(2\omega - \omega_{\text{max}}) + i\Gamma} \tag{5}$$

where ω_{max} corresponds to the peak of the charge-transfer transition energy, $\hbar\omega_{\text{max}}$, Γ is the line width, a and b are wavelength-independent real parameters describing the nonresonant and resonant contributions, respectively, to the nonlinear polarization of the charge-transfer band. Substituting eq 5 into eq 3 and converting frequencies to wavelengths, we obtain

$$\frac{I^{(2\omega)}_{\text{tot}}}{I^{\text{HR}}_{\text{H}_2\text{O}}} - 1 = \left|\sqrt{I^{\text{norm}}_{\text{TiO}_2}(\lambda_{\text{SH}})} + a + \frac{b'}{(\lambda^{-1}_{\text{SH}} - \lambda^{-1}_{\text{max}}) + i\Gamma'}\right|^2 \tag{6}$$

where λ_{max} is the wavelength corresponding to $\hbar\omega_{\text{max}}$, $\Gamma' = \Gamma'/2\pi c$, and $b' = b/2\pi c$ and $I^{\text{norm}}_{\text{TiO}_2}(\lambda_{\text{SH}})$ is the normalized TiO_2 signal, $|E^{\text{SH}}_{\text{TiO}_2}|^2/I^{\text{HR}}_{\text{H}_2\text{O}}$.

Solving for $|E^{\text{norm}}_{\text{cat}-\text{TiO}_2}|$ in eq 3, we get

$$|E^{\text{norm}}_{\text{cat}-\text{TiO}_2}| = \sqrt{\frac{I^{(2\omega)}_{\text{tot}}}{I^{\text{HR}}_{\text{H}_2\text{O}}} - 1 - I^{\text{norm}}_{\text{TiO}_2}\sin^2\varphi} - \cos\varphi\sqrt{I^{\text{norm}}_{\text{TiO}_2}} \tag{7}$$

Hence, to extract $|E^{\text{norm}}_{\text{cat}-\text{TiO}_2}|$, we need, in addition to the two experimentally measurable signals, $I^{(2\omega)}_{\text{tot}}/I^{\text{HR}}_{\text{H}_2\text{O}} - 1$ and $I^{\text{norm}}_{\text{TiO}_2}$, the wavelength-dependent relative phase φ. From the spectrum of the catechol$-TiO_2$ surface complex, the relative phase φ can be calculated at any SH wavelength, using the following equation:

$$\varphi \approx \tan^{-1}\left(\frac{\Gamma'}{\lambda^{-1}_{\text{max}} - \lambda^{-1}_{\text{SH}}}\right) \tag{8}$$

that assumes a is negligible compared to $I^{\text{norm}}_{\text{TiO}_2}(\lambda_{\text{SH}})^{1/2}$, which will be shown later to be valid. To elucidate eq 7, consider two special cases, $\varphi = 0°$ and 90°. If $\varphi = 0°$, e.g., at wavelengths far from resonance, eq 7 reduces to

$$|E^{\text{norm}}_{\text{cat}-\text{TiO}_2}| = \sqrt{\frac{I^{(2\omega)}_{\text{tot}}}{I^{\text{HR}}_{\text{H}_2\text{O}}} - 1} - \sqrt{I^{\text{norm}}_{\text{TiO}_2}} \tag{9}$$

i.e., the total field is simply the sum of the individual fields. If $\varphi = 90°$, which corresponds to the SH wavelength at the resonance peak, λ_{max}, eq 7 reduces to

$$|E^{\text{norm}}_{\text{cat}-\text{TiO}_2}| = \sqrt{\frac{I^{(2\omega)}_{\text{tot}}}{I^{\text{HR}}_{\text{H}_2\text{O}}} - 1 - I^{\text{norm}}_{\text{TiO}_2}} \tag{10}$$

i.e., the total intensity is simply the sum of the individual intensities.

c. SHG Spectrum of the Surface Charge-Transfer Complex. The normalized SH spectra of the TiO_2 suspension and TiO_2 in 1 mM catechol solution are plotted in Figure 3. The spectrum of the TiO_2 suspension was fitted using the second-order polynomial, expression of $I^{\text{norm}}_{\text{TiO}_2}(\lambda_{\text{SH}})$, eq 4. The spectrum of the catechol$-TiO_2$ mixture was then fitted using eq 6 whose $I^{\text{norm}}_{\text{TiO}_2}(\lambda_{\text{SH}})$ term was obtained from the spectrum of the TiO_2 suspension. From eq 6, we obtain the relevant fitting parameters: $\lambda_{\text{max}} = 456 \pm 4$ nm ($\hbar\omega_{\text{max}} = 2.72$ eV), and $\Gamma' = (2.1 \pm 0.5) \times 10^{-4}$ nm^{-1}, corresponding to a linewidth of 45 nm ($\hbar\Gamma = 0.25$ eV), or fwhm $= 90 \pm 20$ nm. The nonresonant part of the catechol$-TiO_2$ charge-transfer response, a, is found to be much smaller than the TiO_2 bulk contribution, $\sqrt{I^{\text{norm}}_{\text{TiO}_2}(\lambda_{\text{SH}})}$, in the wavelength range covered. This conclusion is based on our finding that the fitting of the spectra of the aqueous TiO_2 and catechol$-TiO_2$ suspensions yielded the same value for the nonresonant contribution. Hence, the total SH signal is dominated by the resonant contribution from the charge-transfer band and the nonresonant TiO_2 bulk response.

As noted earlier, Moser et al.[28] and Rodriguez et al.[31] observed a shoulder appearing near 420 nm in both the UV/vis absorbance[28] and diffuse reflectance[31] spectra for the catechol$-TiO_2$ complex. The difference between the results of Rodriguez et al.[31] and the present study may arise from the fact that their diffuse reflectance spectrum were performed on a catechol$-TiO_2$ powder. In the absorbance measurements by Moser et al.[28] an aqueous methanol suspension was used. In both cases, the solvation, the environments of the surface complex, were different from our experimental conditions.

d. Catechol Adsorption Isotherm. The surface complexation is a chemical reaction on the surface, between the solute molecules and the Ti(IV) sites on the surface.[28,31] The surface reaction can be described by

$$\text{M} + \text{ES} \rightleftharpoons \text{FS}$$

where M represents the molecules in the solution, ES represents the empty reaction sites on the surface, and FS represents the filled sites on the surface. Previously, Moser et al.[28] and Rodriguez et al.[31] measured the surface excess, Γ_s, of catechol on colloidal anatase to be 1.0 and 1.25 μmol/m^2, respectively, corresponding to ~170 Å^2 or 130 Å^2 per catechol molecule.

The equilibrium constant of this surface complexation is

$$K_{\text{eq}} = \frac{[\text{FS}]}{[\text{ES}][\text{M}]} \tag{11}$$

If the maximum number of filled surface sites is $[\text{FS}]_{\text{max}}$, the surface coverage θ is defined as

$$\theta = \frac{[\text{FS}]}{[\text{FS}]_{\text{max}}} = \frac{K_{\text{eq}}[\text{M}]}{1 + K_{\text{eq}}[\text{M}]} \tag{12}$$

Since $|E^{\text{norm}}_{\text{cat}-\text{TiO}_2}|$ is proportional to the population of the surface complex on the TiO_2 particles,

$$\theta = \frac{|E^{\text{norm}}_{\text{cat}-\text{TiO}_2}|}{|E^{\text{norm}}_{\text{cat}-\text{TiO}_2}|_{\text{max}}} \tag{13}$$

Combining eqs 12 and 13, one obtains

$$|E^{\text{norm}}_{\text{cat}-\text{TiO}_2}| = \frac{K_{\text{eq}}[\text{M}]}{1 + K_{\text{eq}}[\text{M}]}|E^{\text{norm}}_{\text{cat}-\text{TiO}_2}|_{\text{max}} \tag{14}$$

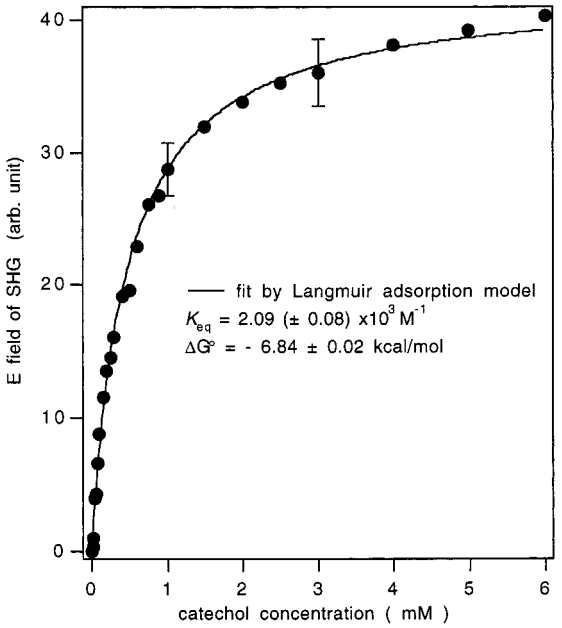

Figure 4. The adsorption isotherm of catechol on TiO_2 particles. For a fundamental laser wavelength of 818 nm, the data points were obtained from the total SH intensity of the mixture and the intensity of TiO_2 alone by eq 7, using the phase difference $\varphi = 40°$. The solid line is a fit to the Langmuir adsorption model, given by eq 14.

In view of eq 7, we can extract the term $|E^{\text{norm}}_{\text{cat}-\text{TiO}_2}|$ that arises from formation of the catechol$-TiO_2$ complex. The concentration of the catechol solution was varied from 0 to 6 mM, and the total SH signal at 409 nm was recorded at each catechol concentration. At concentrations substantially smaller than 1 mM, e.g., in the 10 μM range, the SH signal is monotonic and directly proportional to the bulk catechol concentration, indicating that the relative phase between the surface complex and the TiO_2 bulk signals is positive, i.e., less than 90° at this wavelength. Using the parameters obtained from the spectral fit of Figure 3 and eq 8, one obtains for $\lambda_{SH} = 409$ nm, $\varphi = 40° \pm 10°$. Equation 7 is then employed to obtain the SH field from the surface complex. Figure 4 shows the plot of $|E^{\text{norm}}_{\text{cat}-\text{TiO}_2}|$ as a function of the catechol concentration. An excellent fit to the data of Figure 4, using eq 14, yields $K_{eq} = (2.1 \pm 0.1) \times 10^3\ M^{-1}$, from which the free energy of adsorption is calculated to be $\Delta G° = -6.8$ kcal/mol. This result differs from that of Moser et al., who obtained $K_{eq} = 8 \times 10^4\ M^{-1}$ and $\Delta G° = -9.0$ kcal/mol,[28] and Rodriguez et al., who obtained $K_{eq} = 8 \times 10^3\ M^{-1}$ and $\Delta G° = -7.6$ kcal/mol.[31] We note that our measurements were performed directly on the particles containing the adsorbed molecules, in contrast to the previous experiments where the surface excess was inferred from the amount of loss in the supernatant after the separation stage. In addition to the differences in the methods used to obtain the adsorption isotherms, effects due to the size differences between the nanoparticles and the 0.4 μm particles could be a factor. For instance, the interactions between adsorbates are dependent on the relative adsorbate orientations. Therefore the dipole$-$dipole interactions, for example, could be different for the nanoparticles and the large particles due to the larger curvature of the nanoparticles. At the larger curvature, a decrease in the dipole$-$dipole repulsion would result, and thus contribute to a more negative free energy for the nanoparticles.

4. Conclusions

For the first time, the charge-transfer band of a surface complex formed on TiO_2 colloidal particles is observed using SH spectroscopy. Taking into account the relative phase of the charge-transfer band with respect to the bulk TiO_2 nonlinear responses, we are able to separate these two contributions, thus allowing us to measure the charge-transfer band of the catechol$-TiO_2$ complex, centered at 2.72 eV (456 nm). In addition, the adsorption isotherm of catechol on anatase was obtained in situ using SHG, unlike previous measurements, where a separation procedure was necessary. Our SH measurements yielded an adsorption free energy of $\Delta G° = -6.8$ kcal/mol and an equilibrium constant $K_{eq} = 2.1 \times 10^3\ L\ mol^{-1}$.

Acknowledgment. The authors thank the Division of Chemical Science of the Department of Energy for their support and the National Science Foundation for their equipment support.

References and Notes

(1) Fujishima, A.; Honda, K. *Nature* **1972**, *238*, 37.
(2) Ghosh, A. K.; Maruska, H. R. *J. Electrochem. Soc.* **1977**, *124*, 1516.
(3) Mills, A.; Davies, R. H.; Worsley, D. *Chem. Soc. Rev.* **1993**, 417.
(4) Kurshev, V.; Kevan, L. *Langmuir* **1997**, *13*, 225.
(5) Nakahira, T.; Gratzel, M. *J. Am. Chem. Soc.* **1984**, *88*, 4006.
(6) Gopidas, K. R.; Kamat, P. *J. Phys. Chem.* **1989**, *93*, 6428.
(7) Moser, J.; Gratzel, M. *J. Am. Chem. Soc.* **1984**, *106*, 6557.
(8) Boschloo, G. K.; Goossens, A.; Schoonman, J. *J. Electrochem. Soc.* **1997**, *144*, 1311.
(9) Koffyberg, F. P.; Dwight, K.; Wold, A. *Solid State Commun.* **1979**, *30*, 433.
(10) Vlachopoulos, N.; Liska, P.; Augustynski, J.; Gratzel, M. *J. Am. Chem. Soc.* **1988**, *110*, 1216.
(11) O'Regan, B.; Gratzel, M. *Nature*, **1991**, *353*, 737.
(12) Hashimoto, K.; Hiramoto, M.; Sakata, T. *J. Phys. Chem.* **1988**, *92*, 4272.
(13) Desilvestro, J.; Gratzel, M.; Kavan, L.; Moser, J. *J. Am. Chem. Soc.* **1985**, *107*, 2988.
(14) Kalyanasundaram, K.; Vlachopoulos, N.; Krishnan, V.; Monnier, A.; Gratzel, M. *J. Phys. Chem.* **1987**, *91*, 2342.
(15) Kamat, P. V.; Fox, M. A. *Chem. Rev. Lett.* **1983**, *102*, 379.
(16) Sakata, T.; Hashimoto, K.; Hiromoto, M. *J. Phys. Chem.* **1990**, *94*, 3040.
(17) Kamat, P. V.; Chauvet, J.-P.; Fessenden, R. W. *J. Phys. Chem.* **1986**, *90*, 1389.
(18) Hannappel, T.; Burfeindt, B.; Stork, W.; Willig, F. *J. Phys. Chem. B.* **1997**, *101*, 6799.
(19) Ellingson, R. J..; Asbury, J. B.; Ferrere, S.; Ghosh, H. N.; Sprague, J. R.; Lian, T. Q.; Nozik, A. J. *J. Phys. Chem. B.* **1998**, *102*, 6455.
(20) Heilweil, E. J.; Heimer, T. A. *J. Phys. Chem. B.* **1997**, *101*, 10990.
(21) Tachibana, Y.; Moser, J. E.; Gratzel, M.; Klug, D. R.; Durrant, J. R. *J. Phys. Chem.* **1996**, *100*, 20056.
(22) Itoh, K.; Chiyokawa, Y.; Nakao, M.; Honda, K. *J. Am. Chem. Soc.* **1984**, *106*, 1620.
(23) Liang, Y.; Goncalves, A. M. P.; Negus, D. K. *J. Phys. Chem.* **1983**, *87*, 1.
(24) Rehm, J. M.; McLendon, G. L.; Nagasawa, Y.; Yoshihara, K.; Moser, J.; Gratzel, M. *J. Phys. Chem.* **1996**, *100*, 9577.
(25) Hashimoto, K.; Hiromoto, M.; Lever, A. B. P.; Sakata, T. *J. Phys. Chem.* **1988**, *92*, 1016.
(26) Eichberger, R.; Willig, F. *Chem. Phys.* **1990**, *141*, 159.
(27) Serpone, N.; Lawless, D.; Khairutdinov, R.; Pelizzetti, E. *J. Phys. Chem.* **1995**, *99*, 16655.
(28) Moser, J.; Punchihewa, S.; Infelta, P. P.; Gratzel, M. *Langmuir* **1991**, *7*, 3012.
(29) Houlding, V. H.; Gratzel, M. *J. Am. Chem. Soc.* **1983**, *105*, 5695.
(30) Kalyanasundaram, K.; Neumann-Spallart, M. *J. Phys. Chem.* **1982**, *86*, 5163.
(31) Rodriguez, R.; Blesa, M. A.; Regazzoni, A. E. *J. Colloid Interface Sci.* **1996**, *177*, 122.
(32) Moser, J. E.; Gratzel, M. *Chem. Phys.* **1993**, *176*, 493.
(33) Enea, O.; Moser, J.; Gratzel, M. *J. Electroanal. Chem.* **1989**, *259*, 59.
(34) Martell, E. A.; Smith, R. M. *Critical Stability Constants*, Vol. 3; Plenum: New York, 1976.
(35) Hiemstra, T.; Dewit, J. C.; Riemsdijk, W. *J. Coll. Inter. Sci.* **1989**, *133*, 105.
(36) Wang, H.; Yan, E. C. Y.; Borguet, E.; Eisenthal, K. B. *Chem. Phys. Lett.* **1996**, *259*, 15.
(37) Wang, H.; Yan, E. C. Y.; Liu, Y.; Eisenthal, K. B. *J. Phys. Chem. B* **1998**, *102*, 4446.

(38) Srivastava, A.; Eisenthal, K. B. *Chem. Phys. Lett*. **1998**, *292*, 345.
(39) Zimdars, D.; Yan, E. C. Y.; Liu, Y.; Eisenthal, K. B. Unpublished results.
(40) Yan, E. C. Y.; Eisnethal, K. B. Unpublished results.
(41) Yan, E. C. Y.; Liu, Y.; Eisenthal, K. B. *J. Phys. Chem. B* **1998**, *102*, 6331.
(42) Shen, Y. R. *The Principles of Nonlinear Optics*; Wiley: New York, 1984.
(43) Shultz, A. N.; Hetherington, W. M., III.; Baer, D. R.; Wang L.-Q.; Engelhard, M. H. *Surf. Sci.* **1997**, *392*, 1.
(44) Shultz, A. N.; Jang, Winyann; Hetherington, W. M., III.; Baer, D. R.; Wang L.-Q.; Engelhard, M. H. *Surf. Sci.* **1995**, *339*, 114.
(45) Lantz, J. M.; Baba, R.; Corn, R. M. *J. Phys. Chem.* **1993**, *97*, 7392.
(46) Lantz, J. M.; Corn, R. M. *J. Phys. Chem.* **1994**, *98*, 4899.
(47) Lantz, J. M.; Corn, R. M. *J. Phys. Chem.* **1994**, *98*, 9387.
(48) Berkovic, G.; Shen, Y. R.; Marowsky, G.; Steinhoff, R. *J. Opt. Soc. Am. B* **1989**, *6*, 205.
(49) Schindler, H.; Gamsjager, H. *Faraday Soc. Discussion* **1971**, *52*, 286.
(50) Mo, S.-D.; Ching, W. Y. *Phys. Rev. B* **1995**, *51*, 13023.
(51) Cromer, D. T.; Herrington, K. *J. Am. Chem. Soc*. **1955**, *77*, 4708.
(52) Miller, R. C. *Appl. Phys. Lett.* **1964**, *5*, 17.
(53) Cronemeyer, D. C. *Phys. Rev*. **1952**, *87*, 876.
(54) *Handbook of nonlinear optical crystals*; Dmitriev, V. G., Gurzadyan, G. G., Nikogosyan, D. N., Eds.; Springer-Verlag: Berlin, New York, 1991.
(55) Heinz, T. F. In *Nonlinear Surface Electromagnetic Phenomena*; Ponath, H., Stegeman, G., Eds.; Elsevier: Amsterdam, 1991; p 353.